Applied Microbiology and Biotechnology (2019) 103:8413–8425
https://doi.org/10.1007/s00253-019-10043-6

BIOTECHNOLOGICALLY RELEVANT ENZYMES AND PROTEINS

Growth-coupled evolution of phosphoketolase to improve L-glutamate production by *Corynebacterium glutamicum*

Taiwo Dele-Osibanjo[1,2,3] · Qinggang Li[1,2] · Xiaoli Zhang[1,2] · Xuan Guo[1,2] · Jinhui Feng[1] · Jiao Liu[1,2] · Xue Sun[1,2,3] · Xiaowei Wang[1,2,4] · Wenjuan Zhou[1,2] · Ping Zheng[1,2] · Jibin Sun[1,2] · Yanhe Ma[1]

Received: 5 April 2019 / Revised: 13 July 2019 / Accepted: 23 July 2019 / Published online: 9 August 2019
© Springer-Verlag GmbH Germany, part of Springer Nature 2019

Abstract

The introduction of the key non-oxidative glycolytic (NOG) pathway enzyme, phosphoketolases (PKTs), into heterologous hosts can improve the yield of a variety of acetyl CoA-derived products of interest. However, the low specific activity of existing PKTs compared with that of 6-phosphofructokinase (PFK), the key EMP pathway enzyme, largely limits their potential applications. To improve PKT activity, previous attempts have focused on increasing intracellular PKT concentration via the use of strong promoters. Herein, we report the establishment of a growth-coupled evolution strategy for the enrichment and selection of PKT mutants with improved specific activity in *Corynebacterium glutamicum* hosts with defective PFK. Five mutants from 9 *Bifidobacterium adolescentis*-source PKT (BA-PKT) mutant libraries were obtained. Site-directed mutagenesis analysis revealed 11 mutant sites which contributed to improved BA-PKT specific activity. Further structural analysis revealed that the mutant sites were located far away from the enzyme active site, which makes them almost unpredictable using a rational design approach. Mutant site recombination led to the construction of a novel mutant, $PKT^{T2A/I6T/H260Y}$, with V_{max} 29.77 ± 1.58 U/mg and K_{cat}/K_m 0.32 ± 0.01 s^{-1}/mM, which corresponds to 73.27 ± 3.25% and 80.16 ± 3.38% improvements, respectively, compared with the wildtype (*Vmax*; 17.17 ± 0.59 U/mg, K_{cat}/K_m; 0.17 ± 0.01 s^{-1}/mM). Expression of $PKT^{T2A/I6T/H260}$ in *C. glutamicum* Z188 resulted in 16.67 ± 2.24% and 18.19 ± 0.53% improvement in L-glutamate titer and yield, respectively, compared with the wildtype BA-PKT. Our findings provide an efficient approach for improving the activity of PKTs. Furthermore, the novel mutants could serve as useful tools in improving the yield of L-glutamate and other acetyl CoA-associated products.

Keywords Phosphoketolase · Growth-coupled evolution · Acetyl CoA generation · L-glutamate production · *Corynebacterium glutamicum*

Taiwo Dele-Osibanjo, Qinggang Li and Xiaoli Zhang contributed equally to this work.

Electronic supplementary material The online version of this article (https://doi.org/10.1007/s00253-019-10043-6) contains supplementary material, which is available to authorized users.

✉ Ping Zheng
zheng_p@tib.cas.cn

✉ Jibin Sun
sun_jb@tib.cas.cn

[1] Tianjin Institute of Industrial Biotechnology, Chinese Academy of Sciences, Tianjin 300308, China

[2] Key Laboratory of Systems Microbial Biotechnology, Chinese Academy of Sciences, Tianjin 300308, China

[3] University of Chinese Academy of Sciences, Beijing 100049, China

[4] College of Biotechnology, Tianjin University of Science and Technology, Tianjin 300457, China

Introduction

The native metabolic machinery of most natural microorganisms presents unfavorable atomic economics in biorefinery with respect to the generation of the 2C-compound, acetyl CoA, a central metabolic intermediate and precursor for a range of desirable bioproducts. In the fundamental biochemical infrastructure for sugar catabolism in almost all organisms such as the Embden-Meyerhof-Parnas pathway (EMP) and variants, acetyl CoA is formed through the oxidative decarboxylation of pyruvate. The intrinsic carbon loss associated with this process significantly limits the yield of acetyl CoA-derived products in commonly employed industrial platform strains. Thus, maximizing carbon conservation in bioproduction has received significant attention recently (Keasling 2010; Wang et al. 2018b).

Phosphoketolases (PKTs) (EC 4.1.2.9, EC 4.1.2.22) from the pentose phosphate pathway of lactic acid bacteria and the

D-fructose-6-phosphate (F6P) shunt of *Bifidobacteria*, are versatile tools employed to facilitate carbon conservation in bioproduction. PKTs act in conjunction with phosphotransacetylases and enzymes of the pentose phosphate pathway to catalyze an alternative non-oxidative glycolytic (NOG) pathway with fructose-6-phosphate and/or xylulose-5-phosphate as substrates, bypassing pyruvate decarboxylation and leading to increased generation of stoichiometric amounts of acetyl CoA per glucose molecule (3 mole acetyl CoA/mole glucose compared with 2 mole acetyl CoA/mole glucose obtainable from the conventional pathway) (Bogorad et al. 2013). The application of PKTs in significantly improving the yield of acetyl CoA-associated products such as acetate, acetone, polyhydroxybutyrate, mevalonate, and L-glutamate from a variety of microbial producers has been demonstrated (Bergman et al. 2016; Bogorad et al. 2013; Chwa et al. 2016; de Jong et al. 2014; Henard et al. 2017; Kocharin et al. 2013; Sonderegger et al. 2004; Wang et al. 2018a; Yang et al. 2016). For instance, the expression of PKT in *Corynebacterium glutamicum* has been estimated to improve L-glutamate yield (about 98% by weight) beyond the maximum theoretical yield from the conventional pathway (about 82% by weight) (Chinen et al. 2007). To achieve the 98% yield, the NOG/EMP pathway metabolic flux ratio should be 4:1 (Kozlov et al. 2006). PKTs and 6-phosphofructokinase (PFK) are the key enzymes determining the flux ratio. However, the low activity of characterized PKTs compared with that of PFK significantly limits their potential applications. In most industrial platform strains, the specific enzyme activity of PFK ranges from 148 - 263 U/mg with K_m value between 0.011 – 0.05 mM (Babul 1978; Hofmann and Kopperschlager 1982; Kotlarz and Buc 1982; Nissler et al. 1983; Welch and Scopes 1981), while PKTs from both *Bifidobacteria* and *Lactobacilli* that have been employed in metabolic engineering for improving the yield of acetyl CoA-derived products display specific enzyme activity in the range of 0.7–30 U/mg with K_m value between 1.4 and 39 mM (Grill et al. 1995; Posthuma et al. 2002; Sgorbati et al. 1976; Suzuki et al. 2010b; Yevenes and Frey 2008). Therefore, improving PKT activity is very crucial and can be an effective strategy in metabolic engineering (Henard et al. 2015). Previous attempts have focused on PKT overexpression through the use of strong promoters (Chinen et al. 2007; Henard et al. 2017; Wang et al. 2018b). However, this may increase the cell burden for protein synthesis, and protein overexpression sometimes results in inactive inclusion body formation (Baneyx and Mujacic 2004; García-Fruitós et al. 2005; Gonzalez-Montalban et al. 2005; Strandberg and Enfors 1991). Thus, improving the specific activity of PKTs may be an alternative and better strategy. However, until now, there has been no such report on improving PKT specific activity.

Structure-guided protein rational design and directed enzyme evolution are successful proven approaches in engineering and improving enzyme properties. While rational design requires an in-depth knowledge of enzyme catalytic mechanism, directed evolution offers the possibility of improving enzyme activity without detailed understanding of enzyme structure-function relationships (Bloom et al. 2005; Chen 2001). However, a major challenge in directed evolution is the mutant selection method. Growth-coupled selection has been previously employed to improve the efficiency of directed evolution. For instance, using a growth-coupled evolution strategy, by coupling the xylose utilization ability of the engineered host with the specific activity of xylose isomerase, Lee et al obtained a *Piromyces* sp. xylose isomerase mutant which exhibited 77% increased enzyme activity (Lee et al. 2012). In another instance, Atsumi and Liao obtained several *M. jannaschii* citramalate synthase mutants that led to increased growth of a host auxotrophic for L-isoleucine (Atsumi and Liao 2008).

In this study, a growth-coupled evolution strategy was established for improving the specific activity of PKTs, utilizing *Corynebacterium glutamicum* with defective PFK as hosts, and the industrial relevance of the obtained mutant enzymes in improving the yield of acetyl CoA-derived products with L-glutamate as an example was demonstrated.

Materials and methods

Chemicals and enzymes

Isopropyl-β-D-thiogalactopyranoside (IPTG), L-cysteine hydrochloride, thiamine pyrophosphate, magnesium chloride, xylulose-5-phosphate (X5P), hydroxylamine hydrochloride, trichloroacetic acid, and acetyl phosphate (ACP) were supplied by Sinopharm Chemical Reagent Co. Ltd (Tianjin, China). D-fructose 6-phosphate (F6P) and phosphoenolpyruvate (PEP) were supplied by Solarbio (Beijing, China). 3-morpholinopropanesulfonic acid (MOPS) and adenosine-5′-monophosphate (AMP) were supplied by Amresco (USA). Hexadecyltrimethylammonium bromide (CTAB) and oxaloacetate (OAA) were purchased from Sigma (USA). Adenosine-5′-triphosphate (ATP) was from ThermoFisher Scientific (USA), while erythrose-4-phosphate (E4P) was from Santa Cruz Biotechnology Inc. (USA). Other pure chemicals used in this study were of analytical grade or better. The His SpinTrap columns used for the purification of the PKTs were purchased from GE Healthcare Corporation (USA). DNA polymerase was obtained from Transgene (Beijing, China). Restriction endonucleases were purchased from Fermentas (USA). T4 DNA ligase was purchased from New England Biolabs Inc. (Beijing, China).

Strains and plasmids

The main bacterial strains and plasmids used in this study are listed in Table 1. Other strains and plasmids were constructed based on them. *Escherichia coli* DH5α was used for general cloning and cultivated aerobically at 37 °C in Luria–Bertani (LB) broth. Kanamycin at 50 μg/ml was added to the LB broth as required.

Z188Δ*pfk* and 13032Δ*pfk* were constructed by the knockout of *pfk* gene in Z188 and 13032 via a two-step homologous recombination using the suicide plasmid pK18*mobsacB* according to previously described method (Niebisch and Bott 2001; Schafer et al. 1994). Briefly, the primer pairs Δ*pfk*-F1/Δ*pfk*-R1 and Δ*pfk*-F2/Δ*pfk*-R2 (Table 1) were used to amplify the left and right homologous arms of *pfk* from the genomic DNA of Z188 or 13032, for recombination. The two fragments were capable of annealing to each other by their overlap sequence. The final amplified fragment was digested with *Eco*RI and *Pst*I and inserted into the corresponding sites of pK18*mobsacB*. The resulting plasmid was then introduced into Z188 or 13032 for *pfk* inactivation.

E. coli-C. glutamicum shuttle vector pTRCmob was used for *Bifidobacterium adolescentis*—source PKT (BA-PKT, encoded by *fxpk*) expression in *C. glutamicum* (Liu et al. 2007). The codon-optimized version of *fxpk* was synthesized by Genewiz Company (Suzhou, China) and inserted in pTRCmob vector between *Eco*RI and *Bam*HI sites under the control of the derepressed promoter P_{trc}. The resultant plasmid was named pTR-*fxpk*. To improve the expression of *fxpk*, P_{trc} was mutated by introducing a mutant site using two complementary primers Ptrc-1 and Ptrc-2 (Table 1) to amplify the whole plasmid and through self-recombination, plasmid pTR1-*fxpk* was obtained.

To construct *fxpk* mutant library, a standard error-prone PCR protocol involving the use of *Taq* polymerase with varied concentrations of manganese ions (0.2 mM, 0.5 mM, and 0.8 mM) was employed, using primer pair fxpk-F1/R1 (Table 1) and pTR-*fxpk* as template. The amplified products were mixed, purified, double-digested, and inserted into *Eco*RI and *Bam*HI sites of the pTR-*fxpk* plasmid. Nine parallel libraries were constructed.

For the reintroduction of the *fxpk* mutants PM21, PM41, PM71, PM81, and PM82 into pTR-*fxpk*, fxpk-R1 was used as a common reverse primer for the mutant PCR amplification. The forward primers were PM21-F for PM21, PM41-F for PM41, PM71-F for PM71, PM81/PM82-F for PM81, and PM82, respectively (Table 1). The PCR products were inserted and ligated to replace the wildtype *fxpk* fragment in pTR-*fxpk* after double-digestion with *Eco*RI and *Bam*HI, and purification. With pTR-*fxpk* and the constructed plasmids as templates, fxpk-F1/R2 (Table 1) as primers, PCR was performed to amplify wildtype *fxpk* and selected mutants for ligation into pET30a after double-digestion with *Nde*I and *Xho*I. The constructed pET30a plasmids were used to overexpress PKTs for enzyme analyses.

Site-directed mutagenesis of *fxpk* on plasmids pTR-*fxpk* and pET-*fxpk* was performed. Site mutations were introduced individually into the wildtype gene using a standard procedure involving the PCR amplification of the whole plasmid using complementary primers containing the mutant sites (Table S1) (Miyazaki and Takenouchi 2002). The PCR products were transformed directly into *E. coli* DH5α, and positive transformants were verified and obtained.

To characterize BA-PKT and its mutants, the constructed plasmids were transformed into corresponding hosts, Z188Δ*pfk* or 13032Δ*pfk* for growth analysis, Z188 for L-glutamate production analysis, and BL21 (DE3) for enzyme activity analysis.

Selection of *fxpk* mutant library

The constructed 9 *fxpk* mutant libraries were transferred individually into *E. coli* DH5α cells, each with about 10^4 colonies. After cultivation on LB agar plates, transformants were obtained, scraped off, the plasmids extracted and transformed into Z188Δ*pfk* through electroporation as described previously (Ruan et al. 2015; van der Rest et al. 1999). The Z188Δ*pfk* libraries were allowed to grow for about 48 hours on LBG (LB broth supplemented with 5 g/l glucose) agar plates at 30 °C, before being scraped off and harvested. The process for the enrichment of the positive BA-PKT mutants with improved activities is shown in Fig. 1. The constructed 9 libraries of Z188Δ*pfk* expressing BA-PKT variants were inoculated into 9 wells of a 24-deep-well microtiter plate (each library in one well). Three additional wells were used to cultivate the original Z188Δ*pfk* (pTR-*fxpk*) as control. Each inoculated well contained 1 ml CGXII medium (Keilhauer et al. 1993). Serial transfer was repeated every 48 hours with an inoculum size of 1 % (v/v) cells from the previous culture. After seven rounds of serial transfers, cells from the final culture were plated on solid agar plates, and 3 larger colonies randomly selected from each sample were isolated for further growth analysis in 1 ml CGXII medium in 24 deep-well culture plate. The variants with the highest growth were preliminarily selected. The plasmid vector from the selected variants was purified, the *fxpk* mutants sequenced, ligated into fresh plasmid vector, and retransformed into fresh starting strain background. A second growth rate measurement against the control was performed to confirm that the growth rate improvement was due to the *fxpk* mutants and not background adaptation of the host strain or unwanted mutations on the plasmid backbone. To evaluate cell densities, optical density at 600 nm (OD_{600}) was monitored using a microplate reader (SpectraMax 190 from Molecular Devices, China) with a sample volume of 200 μL.

Table 1 Bacterial strains, plasmids, and primers used in this study

Strain, plasmid, and primer	Relevant characteristic	Reference
Strain		
DH5α	*E. coli*, general cloning host	Takara
BL21 (DE3)	*E. coli*, heterologous protein expression host	Takara
Z188	*C. glutamicum*, GenBank accession number NZ_AKXP00000000, L-glutamate producing strain	Lab stock
13032	Wildtype *C. glutamicum* strain	ATCC
Z188Δ*pfk*	Z188 derivative with its *pfk* deleted	This study
13032Δ*pfk*	13032 derivative with its *pfk* deleted	This study
Plasmid		
pTRCmob	*E. coli-C. glutamicum* shuttle expression vector with a derepressed P_{trc} promoter by deletion of the *lacI* gene, kanamycin resistance	(Liu et al. 2007)
pK18*mobsacB*	Gene deletion/insertion vector, kanamycin resistance	(Schafer et al. 1994)
pET30a	Gene expression vector	Novagen
pTR-*fxpk*	pTRCmob derivative, carries wildtype *fxpk*	This study
pTR-PM21	pTRCmob derivative, carries evolved *fxpk* mutant PM21	This study
pTR-PM41	pTRCmob derivative, carries evolved *fxpk* mutant PM41	This study
pTR-PM71	pTRCmob derivative, carries evolved *fxpk* mutant PM71	This study
pTR-PM81	pTRCmob derivative, carries evolved *fxpk* mutant PM81	This study
pTR-PM82	pTRCmob derivative, carries evolved *fxpk* mutant PM82	This study
pTR-T2A	pTRCmob derivative, carries a site mutant of *fxpk* (T2A)	This study
pTR-I6T	pTRCmob derivative, carries a site mutant of *fxpk* (I6T)	This study
pTR-H260Y	pTRCmob derivative, carries a site mutant of *fxpk* (H260Y)	This study
pTR-T2A/I6T	pTRCmob derivative, carries a double-site mutant of *fxpk* (T2A/I6T)	This study
pTR-T2A/I6T/H260Y	pTRCmob derivative, carries a triple-site mutant of *fxpk* (T2A/I6T/H260Y)	This study
Primer		
Δ*pfk*-F1	CCTCGAATTCGGATGCTGCCAATGGAATGGTGCCCAGTG	This study
Δ*pfk*-R1	CTTCAAGGTTAAATTCATTGCTGGCTGTGC	This study
Δ*pfk*-F2	CAATGAATTTAACCTTGAAGGAAGTCCCATTC	This study
Δ*pfk*-R2	TCTACTGCAGGGAATGATGACACCGATGGTGTCTGTCCTCGAC	This study
fxpk-F1	CTACGAATTCGAAGGAGATATACATATG	This study
fxpk-R1	TCAGGGATCCTCATTCGTTGTCACCCGCGGTC	This study
fxpk-R2	TCAGCTCGAGTTCGTTGTCACCCGCGGTC	This study
Ptrc-1	GAGCGGATAACAATCTCACACAGGAAACAG	This study
Ptrc-2	CTGTTTCCTGTGTGAAATTGTTATCCGCTC	This study
PM21-F	CTACGAATTCGAAGGAGATATACATATGACCTCTCCGGTTACCGGTAC	This study
PM41-F	CTACGAATTCGAAGGAGATATACATATGGCCTCTCCGGTTATCGGTAC	This study
PM71-F	CTACGAATTCGAAGGAGATATACATATGACCTCTCCGGTTATCGGTAC	This study
PM81/PM82-F	CTACGAATTCGAAGGAGATATACATATGACCTCCCCGGTCATCGGTAC	This study

Expression and purification of phosphoketolases

E. coli BL21 (DE3) was used as a protein expression host. The recombinant strains expressing the PKTs were cultivated in LB medium. When the OD_{600} of the culture reached 0.6–0.8, IPTG was added to a final concentration of 0.4 mM. Then, the cultures were cultivated for an additional 18 h at 20 °C. Afterwards, the cells were harvested by centrifugation (4 °C, 7000*g*, 5 min), and washed twice with 30 mL of buffer A (100 mM sodium phosphate buffer, pH 6.5). For protein purification, the cell pellets were resuspended in buffer A and disrupted by sonication (Scientz-IID, Ningbo Scientz Biotech. Co. Ltd). Then, cellular debris was removed by centrifugation at 12,000 rpm and 4 °C for 10 min. The PKT enzyme supernatants with 6 × His fusion tags were purified using His SpinTrap columns, and the bound proteins were eluted with

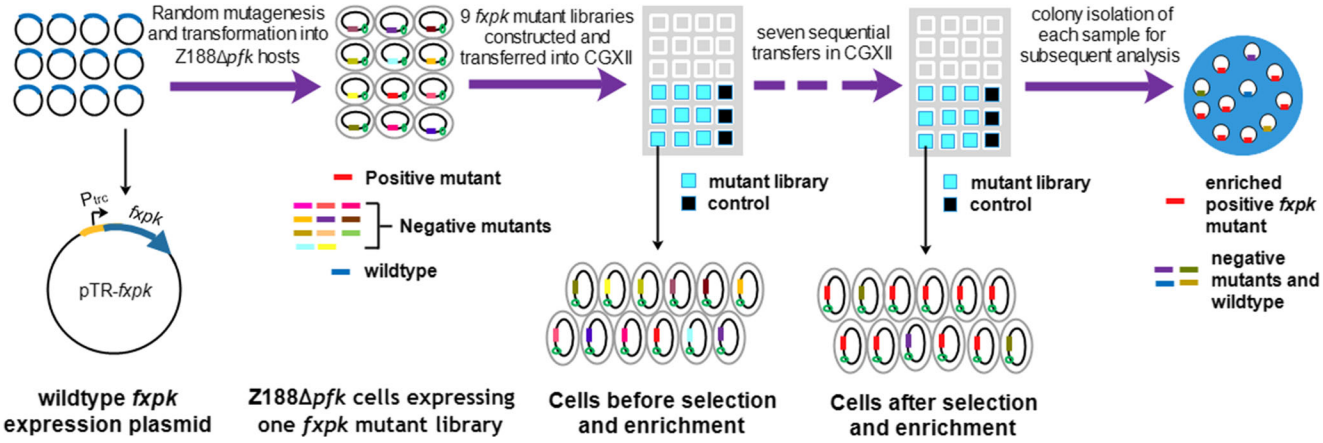

Fig. 1 Workflow of the growth-coupled evolution process for the selection of BA-PKT mutants. Nine BA-PKT mutant libraries were constructed by random mutagenesis. The mutant libraries were individually transformed into host Z188Δ*pfk* cells and serially transferred in CGXII medium in nine wells of 24 deep-well microtiter plate. Three additional wells were used to cultivate the control Z188Δ*pfk* (pTR-*fxpk*) strain expressing wildtype BA-PKT without mutagenesis

concentration-gradient imidazole in buffer A. The pure enzymes were desalted using an Amicon Ultra-4 centrifugal concentrator (10 kDa) at 4 °C and exchanged into buffer B (100 mM sodium phosphate buffer, 1% glycerol, pH 6.5). Enzyme purity was estimated by 12% SDS–PAGE. Protein concentrations were determined according to the method of Bradford (Bradford 1976) using BCA Protein Assay Kit (ThermoFisher Scientific, USA).

Phosphoketolase enzyme activity assay

PKT enzyme activity measurement was through colorimetric assay as reported previously (Meile et al. 2001) with some modifications. The standard reaction mixture of 100 μL comprises sodium phosphate buffer (49 mM, pH 6.5), L-cysteine hydrochloride (0.7 mM), magnesium chloride (0.1 mM), thiamine pyrophosphate (0.1 mM), F6P or X5P as substrate (30 mM), and, finally, the purified enzyme (20 μg) to initiate the reaction. To investigate the effect of tested ligands on PKT activity, E4P, ACP, OAA, and PEP were added to the reaction mixture at a final concentration of 5 mM, respectively, while AMP and ATP were added at a final concentration of 3 mM, respectively. After setting up the reaction, mixing and pre-incubation at 30 °C in a rotary shaker for 10 min, 80 μl of hydroxylamine hydrochloride (2 M) was added and the mixture was further incubated at room temperature for 10 min. Thereafter, 55 μl of 15% (w/v) trichloroacetic acid, 55 μl of 4 M HCl and 55 μl of $FeCl_3.6H_2O$ (5% (w/v) in 0.1 M HCl) were added sequentially for the final ruby color development of the ferric hydroxamate. The generated hydroxamate was spectrophotometrically quantified at 505 nm by comparing with a series of freshly prepared acetyl phosphate standards. One unit of PKT activity is defined as the amount of enzyme forming 1 μmol of acetyl phosphate per minute from F6P or X5P. Specific activity is expressed as units per milligram of protein. PKT activity is expressed in micromoles per minute per milligram of protein.

The kinetic parameters of the purified PKTs for F6P were determined by measuring the activities at different F6P concentrations (0.5–50 mM). The initial-velocity data obtained were fitted to the equation $V = V_{max}[S]/([S] + K_m)$ (where V, initial velocity; V_{max}, maximum velocity; $[S]$, F6P concentration; and K_m, Michaelis constant) by using the GraphPad Prism software (hyperbolic fitting) version 5.

For comparative measurements of crude activity of PKT enzyme in whole *C. glutamicum* cells harboring pTR-*fxpk* and pTR1-*fxpk*, cells were cultured in CGXII for 60 h, harvested by centrifugation (4 °C, 7000*g*, 5 min), washed twice with 30 mL of buffer A, and pretreated with CTAB to release enzymes as reported previously (Orban and Patterson 2000). Enzyme activity was measured using 30 mM F6P as substrate as described above.

L-glutamate production assay

For L-glutamate production, the seed medium contained (l^{-1}) 50 g of glucose, 10 g of $(NH_4)_2SO_4$, 0.8 g of $MgSO_4{\cdot}7H_2O$, 700 μl of H_3PO_4 (v/v), 3 g of corn flour, 10 g of urea, 1 g of tryptone, 0.5 g of yeast extract. The fermentation medium comprises (l^{-1}) 80 g of glucose, 10 g of $(NH_4)_2SO_4$, 0.8 g of $MgSO_4{\cdot}7H_2O$, 700 μl of H_3PO_4 (v/v), 84 g of MOPS, 3 g of corn flour, 10 g of urea. The media were adjusted to pH 7.0 using NaOH.

Seed cultures of Z188 and its derivatives expressing PKT and its mutants were prepared by transferring overnight cultures prepared in LBG medium into 24-deep-well plates containing 1 ml seed medium at an initial OD_{600} of 0.1. Cells at the exponential growth phase were transferred into 1 ml fermentation medium in 24-deep-well plates with an initial OD_{600} of 0.1. The cells were cultivated aerobically at 30 °C

with shaking at 850 rpm for 33 h. The culture supernatant after appropriate dilution, was used for extracellular L-glutamate and residual glucose concentration measurements with the aid of SBA-40D Biosensor Analyzer (Institute of Biology, Shandong Province Academy of Sciences, China) as described previously (Wang et al. 2018c).

Flexible docking

The model structure of the wildtype PKT was constructed with the crystal dimeric structure of *B. longum* PKT (PDB ID: 3AI7) bound to TPP (thiamine pyrophosphate) as template (Takahashi et al. 2010; Zhang and Liu 2013) using Discovery Studio 4.1 software (BIOVIA, formerly Accelrys, USA). The protein active site was determined from PDB site records, and the active site was defined by a sphere of 11-Å radius. Flexible dockings of the ligand F6P into PKT active site were performed with Discovery Studio. Other parameters were kept as default settings in flexible docking.

Nucleotide accession number

The nucleotide sequence for the codon-optimized BA-PKT fragment used in the study had been deposited in GenBank database with the accession number MN081868.

Results

Evolution of phosphoketolase mutants conferring increased Z188Δ*pfk* cell growth in glucose minimal medium

To improve PKT specific activity, in our study, we designed a growth-coupled PKT evolution strategy by inactivating PFK to block the EMP pathway and couple cell growth with PKT activity. We constructed Z188Δ*pfk*, and expressed the wildtype *fxpk* using plasmids pTR-*fxpk* and pTR1-*fxpk*, with promoters P_{trc} and its mutant promoter where part of the P_{trc} sequence was replaced resulting in increased strength (TAACAAT**T**TCACACA changed to TAACAAT**C**TCAC ACA). We then compared the growths of Z188, Z188Δ*pfk*, Z188Δ*pfk* (pTR-*fxpk*), and Z188Δ*pfk* (pTR1-*fxpk*) in CGXII medium. As shown in Fig. 2a, the OD_{600} of Z188Δ*pfk* (pTR1-*fxpk*) at 60 h was about 1.4 fold higher compared with that of Z188Δ*pfk* (pTR-*fxpk*). The growth rate of the unmodified parent strain was much higher (exceeded 14 fold, from 4 h to 12 h) than Z188Δ*pfk* (pTR1-*fxpk*). Moreover, at 60 h, the P_{trc} mutant led to about 1.5-fold improvement in PKT crude activity (Z188Δ*pfk* (pTR1-*fxpk*); 12.46 ± 0.34 U/OD_{600} vs Z188Δ*pfk* (pTR-*fxpk*); 8.36 ± 0.34 U/OD_{600}). The results indicate that the growth of Z188Δ*pfk* can be coupled to the level of BA-PKT enzyme activity under the designed experimental condition in our study. Moreover, the large growth gap between the parent strain Z188 and Z188Δ*pfk* strain with significantly increased expression of PKT implies an immense potential for enhancing PKT enzyme activity.

To apply the growth-based evolution strategy in selecting better PKT mutants, pTRCmob was used to construct nine parallel *fxpk* mutant libraries each with about 10^4 variants. The libraries were transformed into Z188Δ*pfk*. Selection of mutants on the basis of growth improvement was thereafter carried out. The pools of cells from the mutant library were serially subcultured in CGXII medium for seven transfers. The growth rates for the pools of cells from the PKT mutant library (M1-M9) compared with the strain expressing the wildtype PKT are shown in Fig. 2b. It was observed that the growth of strains from M2, M4, M7, and M8 progressively improved during the evolution process. Following the selection process, mutant strains from these four libraries were subcultured on solid CGXII media plates for single colony isolation. Three colonies with large sizes were randomly selected from each library and further tested for growth (Fig. 2c). The *fxpk* mutants from two strains with better growth among the three selected colonies of each sample were sequenced. Except for M81 and M82, the other sequenced mutant *fxpk* fragments from the same library were the same (Fig. 2c and Table 2).

To eliminate the possibility of any adaptive changes which may arise from the genomic DNA and plasmid of the selected strains in the course of the evolution, the *fxpk* genes from mutants M21, M41, M71, M81, and M82 (Fig. 2c) were amplified with a high-fidelity DNA polymerase and cloned into pTR-*fxpk* (substituting original *fxpk*). The freshly constructed expression plasmids were retransformed into Z188Δ*pfk* host strain with clean background. The growth curves of the retransformed strains (M21N, M41N, M71N, M81N, and M82N) in CGXII medium are shown in Fig. 2d. From the observed growth rate, it was evident that the PKT mutants improved the growth of the host strain.

Enzyme assay of evolved phosphoketolase mutants

To understand the basis for the growth improvement conferred by the evolved phosphoketolase mutants on Z188Δ*pfk* in CGXII medium, in vitro BA-PKT enzyme assay was conducted on the pure enzymes using a colorimetry-based coupled enzyme assay system as reported previously (Meile et al. 2001). Since the BA-PKT used in this study is dual-substrate specific for F6P and X5P, we compared the activity of the wildtype enzyme using X5P or F6P as substrates. The wildtype enzyme displayed much higher activity towards F6P (12.07 ± 0.09 U/mg) compared with X5P (0.04 ± 0.00 U/mg) up to 302-fold, implying that the BA-PKT employed in this study displays higher substrate affinity towards F6P. This observation is consistent with a previous report in which the

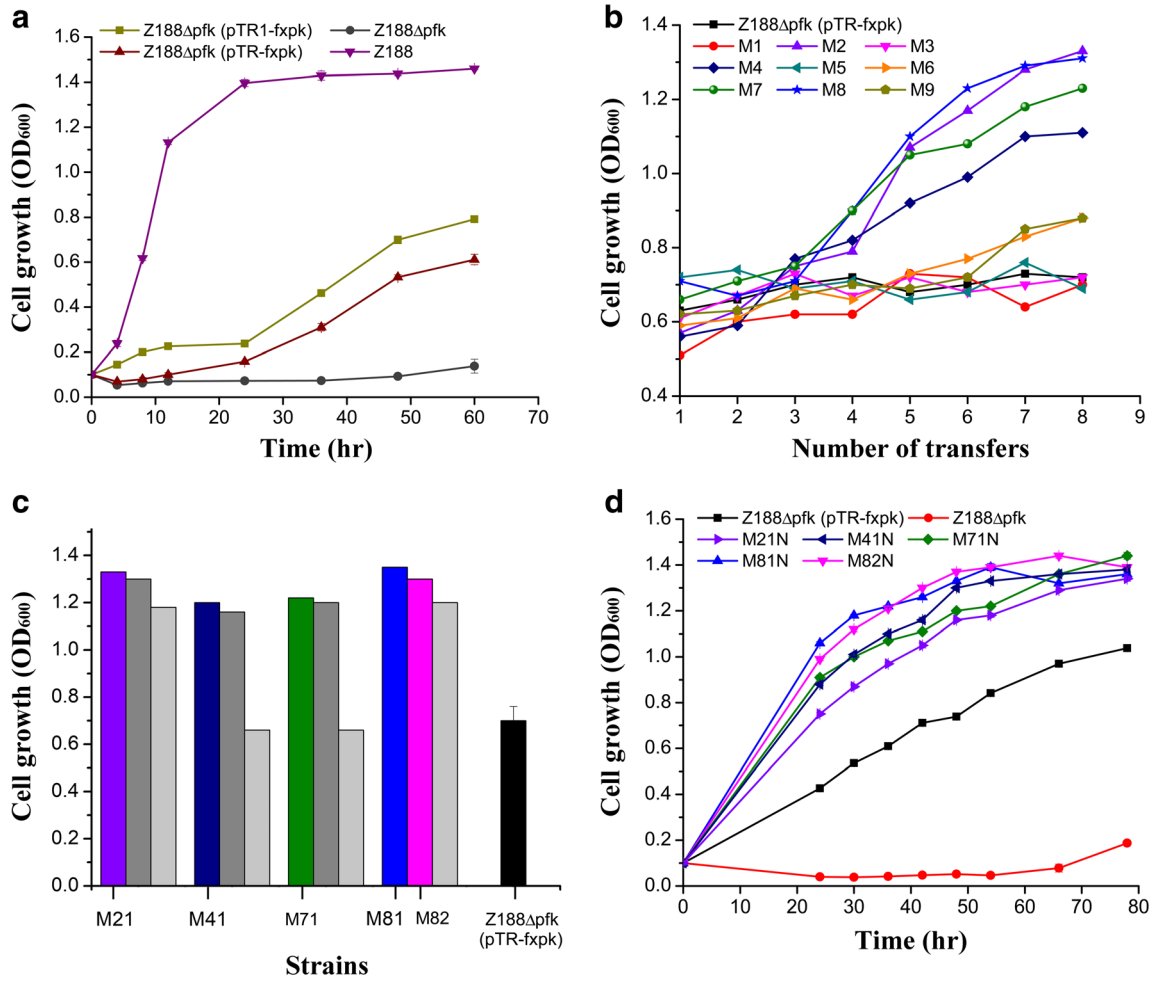

Fig. 2 Growth-coupled selection process for phosphoketolase mutants. **a** Comparison of cell growth of strains Z188, Z188Δ*pfk*, and Z188Δ*pfk* expressing wildtype BA-PKT with native P_{trc} promoter (Z188Δ*pfk* (pTR-*fxpk*)) and mutant P_{trc} promoter with increased strength (Z188Δ*pfk* (pTR1-*fxpk*)). **b** Growth-based selection of BA-PKT mutants. Cultures were serially transferred seven times in CGXII medium for strain enrichment. M1-M9; pools of cells from BA-PKT mutant library. Four cultures M2, M4, M7, and M8 were selected for further analyses based on their improved growth. **c** Growth assay of 3 clones selected from each of the 4 evolved BA-PKT mutant cultures. Based on sequence analyses, M21, M41, M71, M81, and M82 were selected for further analyses. **d** Growth curves for the reconstructed strains (M21N, M41N, M71N, M81N and M82N) expressing the selected BA-PKT mutants

activity of X5P/F6P phosphoketolase was found to be much higher for F6P compared with X5P (Servinsky et al. 2012). In addition, the activities of five mutants with X5P as substrate were still a hundred-fold lower than the corresponding activities with F6P as substrate (Table S2). Since both F6P and X5P act as substrates for PKTs and facilitate the same theoretical yield improvement of acetyl CoA-derived products via the NOG pathway (Bogorad et al. 2013), and due to the

Table 2 Nucleotide and amino acid changes identified in BA-PKT mutants

Phosphoketolase mutant	Nucleotide change(s)	Amino acid change(s)
PM21	T17C$^{(2)}$, T2133C$^{(-)}$, A358G$^{(5)}$, G691A$^{(6)}$ A1190G$^{(9)}$, A1230G$^{(-)}$, A2027G$^{(12)}$	I6T$^{(2)}$, T120A$^{(5)}$, E231K$^{(6)}$ K397R$^{(9)}$, D676G$^{(12)}$.
PM41	A4G$^{(1)}$, A147G$^{(-)}$, T1251C$^{(-)}$, T1656C$^{(-)}$, T1737C$^{(-)}$, T2016C$^{(-)}$, T2353C$^{(13)}$	T2A$^{(1)}$, F785L$^{(13)}$
PM71	A40G$^{(3)}$, G1481A$^{(11)}$, T2401C$^{(14)}$; C2374T$^{(-)}$	N14D$^{(3)}$, R494H$^{(11)}$, W801R$^{(14)}$
PM81	T9C$^{(-)}$, T15C$^{(-)}$, A60T$^{(4)}$, C778T$^{(7)}$, G1024A$^{(8)}$, G1401A$^{(10)}$	E20D$^{(4)}$, H260Y$^{(7)}$, E342K$^{(8)}$, M467I$^{(10)}$
PM82	T9C$^{(-)}$, T15C$^{(-)}$, A60T$^{(4)}$, C778T$^{(7)}$, G1024A$^{(8)}$	E20D$^{(4)}$, H260Y$^{(7)}$, E342K$^{(8)}$

$^{(1)}$-$^{(14)}$ Nucleotide substitutions and corresponding amino acid mutations

$^{(-)}$ Base substitutions with no corresponding amino acid changes

much lower specific enzyme activity recorded from X5P, F6P was chosen as the substrate for the enzyme assays conducted thereafter. As shown in Fig. 3, in a similar trend observed with the growth rate, the specific enzyme activities of the PKT mutants improved significantly.

The cumulative amino acid substitutions identified in the mutants were analyzed to identify the ones that are essential for the improved activity of the mutant BA-PKTs. To accomplish this, single mutations of each amino acid substitution were introduced into the wildtype BA-PKT, and the resulting single-site mutants were expressed and purified and their enzyme activities evaluated with 30 mM F6P as substrate. The SDS-PAGE bands of the representative PKTs which showed that they were of high purity and correspond to the reported 90-kDa molecular weight (Chinen et al. 2007; Henard et al. 2017; Meile et al. 2001) are shown in Fig. S1. From the enzyme assay results (Fig. 3), 11 of the 14 tested single-site mutants showed improved activity. The best three PKTs with mutations at position 2 (T2A), position 6 (I6T), and position 260 (H260Y), yielded 32.81 ± 0.50%, 44.10 ± 7.46%, and 52.41 ± 5.07% increased specific activities compared with the wildtype. This suggests that these three mutations contribute significantly to the improved activity of the BA-PKT mutants. To determine whether the combination of these three mutations will yield a synergistic effect on improved PKT activity, double and triple site mutations were introduced into the wildtype. As depicted in Fig. 3, the combined double (T2A/I6T) and triple mutations (T2A/I6T/H260Y), resulted in much more improved enzyme activity compared with single amino acid substitution at the respective sites, exhibiting 75.54 ± 3.00% and 76.37 ± 2.33% increased enzyme activities, respectively, compared with the wildtype. Notably, we observed that the combined mutations of the three site mutants (T2A/I6T/H260Y) did not yield a significant increase in the PKT specific activity compared with the double mutant (T2A/I6T), although the single-site mutant (H260Y) yielded significantly increased specific activity compared with the wildtype. The underlying reason for this observation seems to be complicated.

Kinetics analysis of phosphoketolase mutants

Since the three PKT mutants H260Y, T2A/I6T, and T2A/I6T/H260Y yielded the best improvement in enzyme activity (Fig. 3), they were selected for further kinetics analysis. Their V_{max} values displayed 48.96 ± 7.40%, 59.12 ± 4.84% and 73.27 ± 3.25% respective increases more than the wildtype (Table 3). The K_{cat}/K_m values of these mutant enzymes also improved significantly, with 60.34 ± 7.97%, 71.45 ± 5.22% and 80.16 ± 3.38% increases over that of the wildtype. The K_m values of both the wildtype and mutant enzymes compare with previous reports (Bogorad et al. 2013; Meile et al. 2001). It is also noteworthy that there was no significant change in the K_m values for the mutant enzymes compared with the wildtype, implying that both the mutant enzymes and the wildtype may demonstrate similar affinities towards F6P. To study the possible mechanism underlying the enzyme kinetics change, we built a model structure for the BA-PKT in this study with TPP as co-factor and performed the flexible dockings of the ligand F6P into the BA-PKT. As shown in Fig. S2, the F6P interacts with TPP at the enzyme active site pocket, but the mutant sites were far away from the active center. This may provide some explanation for the observed insignificant change in the K_m of the mutant enzymes compared with the wildtype, with changes reflecting only in the respective V_{max} values.

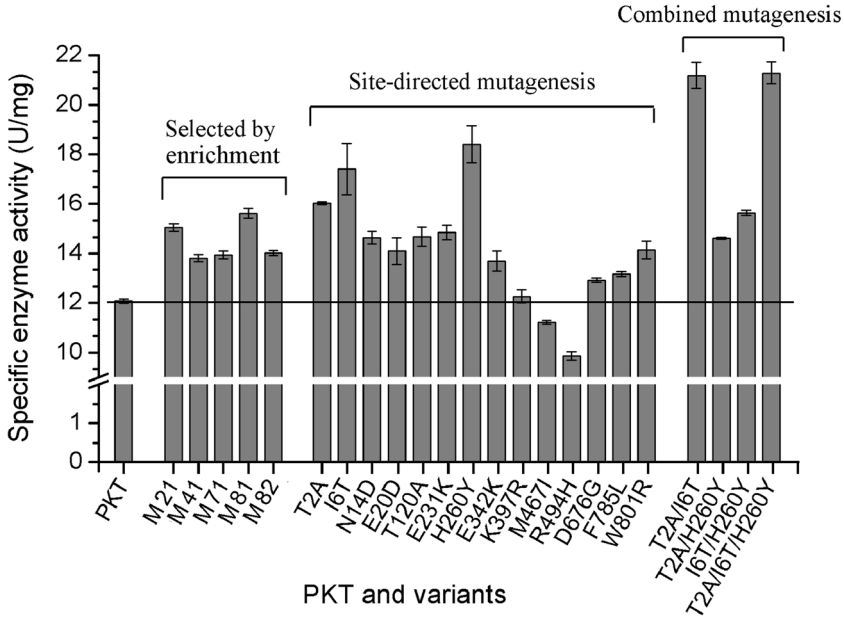

Fig. 3 Enzyme activity assay of both evolved and constructed BA-PKT mutants with F6P as substrate. M21, M41, M71, M81, and M82 represent the BA-PKT mutants from the corresponding strains. For other mutants, the mutant sites are indicated. The F6P concentration was 30 mM. Error bars indicate standard deviation from three independent measurements

Table 3 Kinetic constants of purified BA-PKT and mutants

Phosphoketolase	V_{max} (U/mg)	K_m (mM)	K_{cat} (s^{-1})	K_{cat}/K_m (s^{-1}/mM)
BA-PKT	17.17 ± 0.59	9.96 ± 0.98	1.73 ± 0.12	0.17 ± 0.01
H260Y	25.62 ± 2.15	9.86 ± 2.44	2.71 ± 0.45	0.28 ± 0.02
T2A/I6T	27.35 ± 1.77	9.73 ± 1.87	2.88 ± 0.37	0.30 ± 0.02
T2A/I6T/H260Y	29.77 ± 1.58	9.84 ± 1.53	3.07 ± 0.32	0.32 ± 0.01

The values shown indicate mean ± standard deviation from three parallel experiments. Determination of K_m and V_{max} for wildtype and PKT mutants was performed using varied F6P concentrations as substrates at 30 °C and pH 6.5

Phosphoketolase mutants enhance L-glutamate yield

To demonstrate the potential of the mutant BA-PKTs in improving the production of acetyl CoA-derived products, we tested their effects on L-glutamate yield. Strain Z188 (pTR-*fxpk*) and its derivatives expressing the enriched BA-PKT mutants, the best three single-site mutants and the best two site-combined mutants, were constructed. The L-glutamate production and cell growth were tested in 24-deep-well culture plate. As shown in Fig. S3, no significant difference was observed in the growth rates of the tested strains. As illustrated in Fig. 4, in agreement with previous studies which improved the yield of acetyl CoA-associated products by PKT overexpression, utilizing the promoter P_{trc} to express the wildtype BA-PKT, the L-glutamate yield increased by 9.02 ± 0.66%, compared with the strain without PKT. With the use of the mutant PKTs, L-glutamate titer and yield further increased to varying levels, with the triple mutant enzyme, T2A/I6T/H260Y displaying the highest percentage increase of 16.67 ± 2.24% and 18.19 ± 0.53%, respectively, compared with the wildtype BA-PKT. The results indicate that in addition to PKT overexpression, the obtained best PKT mutant with improved specific activity can highly enhance the production of L-glutamate. To further improve the L-glutamate yield from the PKT mutants, fermentation in jar reactors under optimized conditions is recommended in the future.

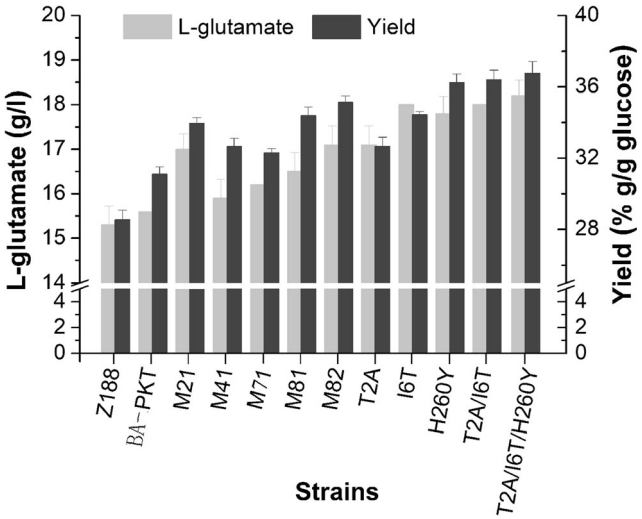

Fig. 4 L-glutamate production assay of Z188 and its derivatives expressing BA-PKT variants. L-glutamate production titers (gray bars) and L-glutamate yield (black bars). PKT, M21, M41, M71, M81, and M82 represent Z188 derivatives expressing the corresponding PKT variants. For Z188 derivatives expressing other mutant BA-PKTs, the mutant sites are indicated. Error bars indicate standard deviation from three independent measurements. Cells were cultured for 33 hours before L-glutamate production was quantified

Discussion

PKTs are promising enzymes for improving the production of a range of beneficial acetyl CoA-associated products. However, a significant factor limiting their potential applications lies in their low specific activities compared with that of PFK. Previous strategies employed strong promoters to improve PKT expression level (Bogorad et al. 2013; Chinen et al. 2007; Kocharin et al. 2013; Krusemann et al. 2018; Wang et al. 2018b). As a result, intracellular concentrations of the enzyme were increased and the yields of target acetyl CoA-associated products were significantly improved. For instance, by overexpressing BA-PKT in *Escherichia coli*, Bogorad et al. improved acetate yield from xylose by 500% (Bogorad et al. 2013). Similarly, by overexpressing PKT from *Aspergillus nidulans* in *Saccharomyces cerevisiae*, Kocharin et al. improved the yield of polyhydroxybutyrate from glucose by 50% (Kocharin et al. 2013). However, these studies failed to address the challenge of PKT low specific activity, which is the central focus of this study.

To improve the specific activity of enzymes, structure-guided protein design and directed enzyme evolution are two major enabling technologies widely applied. Rational protein design approach focuses on modification of residues located at or close to the enzyme active site, residues located at protein interfaces and residues which play important roles in stabilization of protein conformations, to generate new enzymes with improved functions (Bloom et al. 2005; Chen 2001). The demerit of this strategy is that it requires an exhaustive knowledge of enzyme active sites and structure-function relationships. Directed evolution on the other hand screens and selects new enzymes of desired functions from a constructed library of the parent protein, and thus do not

require detailed protein structural and functional data. The application of growth-coupled evolution as an effective approach in selecting new enzymes of improved activity and other desirable characteristics had been demonstrated previously (Atsumi and Liao 2008; Lee et al. 2012; Liu et al. 2018; Pan et al. 2013). The key is to effectively couple the cell growth of the engineered strain solely to the activity of the target enzyme. In this study, by deleting *pfk* in Z188, carbon flux through the EMP pathway should be reduced and rerouted by heterologously expressed BA-PKT towards the alternative NOG pathway. Through this installed mechanism, a platform is created for coupling strain growth to improved BA-PKT activity. By means of evolution in glucose minimal medium, the obtained BA-PKT mutants were all confirmed by reintroduction into host cells, to be positively coupled with increased host cell growth (Fig. 2d), and the specific enzyme activities of all the tested PKT mutants improved significantly (Fig. 3), indicating the high efficiency of the established growth coupled PKT directed evolution strategy in our study. The growth-coupled evolution strategy was also tested in the model *C. glutamicum* strain ATCC 13032. Similar results as recorded for Z188 were obtained (Fig. 2a and Fig S4). This confirms that the PKT evolution strategy should also be applicable in other commonly accessible *C. glutamicum* model strains.

As a result of the installed growth-coupled evolution strategy, 5 better BA-PKT mutants M21, M41, M71, M81, and M82 were obtained. To determine if the mutants affected parameters such as feedback inhibition or allosteric activation, we investigated the function of 6 potential effectors E4P, ACP, OAA, PEP, ATP, and AMP on the enzymatic activities of wildtype BA-PKT and its mutants. E4P and ACP, the products of the reaction catalyzed by BA-PKT with F6P as substrate, were found to have an insignificant feedback inhibition effect on BA-PKTs' activity (Fig. S5a). No previous report assessed the effects of E4P and ACP on PKT activity. As OAA, PEP, ATP, and AMP had been previously reported as the allosteric regulators of PKTs from both bacterial and eukaryotic origin (Glenn et al. 2014; Glenn and Smith 2015), their effects on both wildtype and mutant BA-PKTs isolated in this study were tested (Fig. S5). Less than 15% of BA-PKTs' activity was reduced by 5 mM PEP, whereas 40% activities of both *C. neoformans* Xfp2 and *L. plantarum* Xfp were inhibited. The BA-PKTs were neither sensitive to 5 mM OAA, which is identical to *L. plantarum* Xfp; however, the activity of *C. neoformans* Xfp2 was inhibited by 50%. The BA-PKTs retained about 60% of the activity at 3 mM ATP, whereas only about 10% activity of *C. neoformans* Xfp2 was retained in the presence of 3 mM ATP, and *R graminis* Xfp activity was totally inhibited at 0.1 mM ATP (Glenn et al. 2014; Glenn and Smith 2015; Whitworth and Ratledge, 1977). AMP is an allosteric activator of *C. neoformans* Xfp2 activity; however, 3 mM AMP did not demonstrate a significant effect on BA-PKTs and *L. plantarum* Xfp's activities. Altogether, the wildtype and mutant BA-PKTs are better than previously reported enzymes in resistance to inhibition by the six tested effectors. The overall effect of the mutant sites on the BA-PKT activity in the presence of the tested metabolites seemed not to be significant with the exception of ATP, which showed an observable different effect on the BA-PKTs.

Subsequent mutant site analysis of the BA-PKT mutants led to the construction of mutants, T2A, I6T, H260Y, T2A/I6T, and T2A/I6T/H260Y with 32.81 ± 0.50%, 44.10 ± 7.46%, 52.41 ± 5.07%, 75.54 ± 3.00% and 76.37 ± 2.33% respective improved specific enzyme activities compared with the codon-optimized wildtype BA-PKT (12.07 ± 0.09 U/mg). Kinetic analysis of the best three mutants H260Y, T2A/I6T, and T2A/I6T/H260Y revealed the V_{max} values between 25–29 U/mg, and the K_m values of 9.7–9.9 mM. Compared with the previously reported PKTs often employed in metabolic engineering, especially PKTs from *B. adolescentis* (Specific activity; 0.7 U/mg), *B. animalis* (Specific activity; 4.28 U/mg, K_m; 10 mM), *B. breve* (Specific activity; 14.0 U/mg, K_m; 9.7 mM), *B. longum* (Specific activity; 14.6 U/mg, K_m; 26 mM) and *L. plantarum* (Specific activity; 1.8 U/mg, K_m; 24 mM) activities for F6P (Bogorad et al. 2013; Grill et al. 1995; Meile et al. 2001; Suzuki et al. 2010a; Yevenes and Frey 2008), the best three codon-optimized BA-PKT mutants obtained in our study, especially T2A/I6T/H260Y, might serve as better candidates for metabolic engineering.

Based on the catalytic mechanism of PKTs as proposed previously, the N-terminal domain (residues 2–378) and the middle domain (residues 379–612) interact with the cofactor TPP and the substrate, F6P to facilitate the catalytic mechanism. The reported key enzyme active site residues are His64, His97, Gly155, Glu479, and His553, respectively (Suzuki et al. 2010a; Takahashi et al. 2010; Zhang and Liu 2013). In our efforts to understand the basis for the improved specific activities of the BA-PKT mutants, we constructed the 3D model structure of BA-PKT based on the crystal structure of *B. longum* phosphoketolase (PDB ID: 3AI7 (Takahashi et al. 2010; Zhang and Liu 2013)) which shows 59% amino acid sequence similarity. From our analysis, we discovered that all of the mutations including the mutants with higher activities (principally T2A, I6T, and H260Y) were located far away from the enzyme active site, and no clear interaction was disclosed by our preliminary structure analysis (Fig. S2). Therefore, the residues are generally hard to be predicted by structure-based rational design strategy, suggesting that directed evolution approach is a powerful alternative for the study of enzyme structure-function relationship. It deserves to mention that of the 11 beneficial mutant sites found in this study, 4 were located within the first 20 amino acids of the N-terminal domain of the protein. Moreover, two mutants out of the 4 residues, T2A, I6T, together with the double mutant, T2A/I6T

displayed significantly improved enzyme activities, indicating the potential important contribution of the short sequence to the enzyme function.

To demonstrate the applicability of the BA-PKT mutants in improving the production of acetyl CoA-associated products, we tested their effects on L-glutamate production by Z188. Previously, by overexpressing PKT from *B. animalis* JCM1190 using the strong constitutively active *cspB* promoter (Peyret et al. 1993) in *C. glutamicum*, the L-glutamate yield of the strain improved by 9% (Chinen et al. 2007). In this study, using P_{trc} for expressing wildtype BA-PKT in Z188, L-glutamate yield improved by 9.02 ± 0.66%, which is in agreement with the improved yield reported previously as a result of PKT overexpression (Wang et al. 2018b; Yang et al. 2016). However, with the expression of the best BA-PKT mutant T2A/I6T/H260Y, L-glutamate yield further improved by 18.19 ± 0.53% (Fig. 4). The results indicate that improving the specific activity of PKTs is a promising strategy for improving acetyl CoA-associated metabolites production.

In summary, in this study, we established an efficient growth-coupled evolution strategy for significantly improving the activities of PKTs in *C. glutamicum*, leading to better yield of L-glutamate. To further improve the specific activity of the PKT mutants to a comparable ratio to that of PFK, the key enzyme of the competing pathway, further rounds of growth-coupled evolution should be conducted. For the aim of enhanced yield of target products, optimization of downstream pathway to form a strong flux pulling force, coupled with optimization of the fermentation conditions is recommended. The established strategy can be also applied for improving the performance of other metabolism limiting enzymes for target applications.

Acknowledgments We thank Guoqiang Cao and Zijian Tan (both from Tianjin Institute of Industrial Biotechnology, Chinese Academy of Sciences) for technical support in Z188Δ*pfk* strain construction and BA-PKT 3-D structure analysis, respectively.

Funding information This research was supported by grants from the National Natural Science Foundation of China (31870081), the National Key R&D Program of China (2018YFA0901403), the Special Program of Talents Development for Excellent Youth Scholars in Tianjin (TJTZJH-QNBJRC-2-10), the Youth Innovation Promotion Association of Chinese Academy of Sciences (2016164), and the Science and Technology Project of Tianjin (15PTCYSY00020 and 14ZCZDSY00157).

Compliance with ethical standards This article does not contain studies with human participants or animals performed by any of the authors. All authors confirm that ethical principles have been followed in the research as well as in manuscript preparation, and approved this submission

Conflict of interest The authors declare that they have no conflict of interest.

References

Atsumi S, Liao JC (2008) Directed evolution of *Methanococcus jannaschii* citramalate synthase for biosynthesis of 1-propanol and 1-butanol by *Escherichia coli*. Appl Environ Microbiol 74(24): 7802–7808. https://doi.org/10.1128/aem.02046-08

Babul J (1978) Phosphofructokinases from *Escherichia coli*. Purification and characterization of the non-allosteric isozyme. J Biol Chem 253(12):4350–4355

Baneyx F, Mujacic M (2004) Recombinant protein folding and misfolding in *Escherichia coli*. Nat Biotechnol 22(11):1399–1408. https://doi.org/10.1038/nbt1029

Bergman A, Siewers V, Nielsen J, Chen Y (2016) Functional expression and evaluation of heterologous phosphoketolases in *Saccharomyces cerevisiae*. AMB Express 6:13. https://doi.org/10.1186/s13568-016-0290-0

Bloom JD, Meyer MM, Meinhold P, Otey CR, MacMillan D, Arnold FH (2005) Evolving strategies for enzyme engineering. Curr Opin Struct Biol 15(4):447–452. https://doi.org/10.1016/j.sbi.2005.06.004

Bogorad IW, Lin TS, Liao JC (2013) Synthetic non-oxidative glycolysis enables complete carbon conservation. Nature 502(7473):693–698. https://doi.org/10.1038/nature12575

Bradford MM (1976) Rapid and sensitive method for quantitation of microgram quantities of protein utilizing principle of protein-dye binding. Anal Biochem 72(1-2):248–254. https://doi.org/10.1006/abio.1976.9999

Chen RD (2001) Enzyme engineering: rational redesign versus directed evolution. Trends Biotechnol 19(1):13–14. https://doi.org/10.1016/s0167-7799(00)01522-5

Chinen A, Kozlov YI, Hara Y, Izui H, Yasueda H (2007) Innovative metabolic pathway design for efficient L-glutamate production by suppressing CO_2 emission. J Biosci Bioeng 103(3):262–269. https://doi.org/10.1263/jbb.103.262

Chwa JW, Kim WJ, Sim SJ, Um Y, Woo HM (2016) Engineering of a modular and synthetic phosphoketolase pathway for photosynthetic production of acetone from CO_2 in *Synechococcus elongatus* PCC 7942 under light and aerobic condition. Plant Biotechnol J 14(8): 1768–1776. https://doi.org/10.1111/pbi.12536

de Jong BW, Shi S, Siewers V, Nielsen J (2014) Improved production of fatty acid ethyl esters in *Saccharomyces cerevisiae* through up-regulation of the ethanol degradation pathway and expression of the heterologous phosphoketolase pathway. Microb Cell Factories 13:10. https://doi.org/10.1186/1475-2859-13-39

García-Fruitós E, González-Montalbán N, Morell M, Vera A, Ferraz RM, Arís A, Ventura S, Villaverde A (2005) Aggregation as bacterial inclusion bodies does not imply inactivation of enzymes and fluorescent proteins. Microb Cell Factories 4:27. https://doi.org/10.1186/1475-2859-4-27

Glenn K, Smith KS (2015) Allosteric Regulation of *Lactobacillus plantarum* Xylulose 5-Phosphate/Fructose 6-Phosphate Phosphoketolase (Xfp). J Bacteriol 197(7):1157–1163. https://doi.org/10.1128/jb.02380-1

Glenn K, Ingram-Smith C, Smith KS (2014) Biochemical and kinetic characterization of xylulose 5-phosphate/fructose 6-phosphate phosphoketolase 2 (Xfp2) from *Cryptococcus neoformans*. Eukaryot Cell 13(5):657–663. https://doi.org/10.1128/EC.00055-14

Gonzalez-Montalban N, Carrio MM, Cuatrecasas S, Aris A, Villaverde A (2005) Bacterial inclusion bodies are cytotoxic in vivo in absence of functional chaperones DnaK or GroEL. J Biotechnol 118(4):406–412. https://doi.org/10.1016/j.jbiotec.2005.05.024

Grill JP, Crociani J, Ballongue J (1995) Characterization of fructose 6 phosphate phosphoketolases purified from *Bifidobacterium* species. Curr Microbiol 31(1):49–54

Henard CA, Freed EF, Guarnieri MT (2015) Phosphoketolase pathway engineering for carbon-efficient biocatalysis. Curr Opin Biotechnol 36:183–188. https://doi.org/10.1016/j.copbio.2015.08.018

Henard CA, Smith HK, Guarnieri MT (2017) Phosphoketolase overexpression increases biomass and lipid yield from methane in an obligate methanotrophic biocatalyst. Metab Eng 41:152–158. https://doi.org/10.1016/j.ymben.2017.03.007

Hofmann E, Kopperschlager G (1982) Phosphofructokinase from yeast. Methods Enzymol 90(Pt E):49–60

Keasling JD (2010) Manufacturing molecules through metabolic engineering. Science 330(6009):1355–1358. https://doi.org/10.1126/science.1193990

Keilhauer C, Eggeling L, Sahm H (1993) Isoleucine synthesis in *Corynebacterium-glutamicum* - Molecular analysis of the ilvB-ilvN-ilvC operon. J Bacteriol 175(17):5595–5603

Kocharin K, Siewers V, Nielsen J (2013) Improved polyhydroxybutyrate production by *Saccharomyces cerevisiae* through the use of the phosphoketolase pathway. Biotechnol Bioeng 110(8):2216–2224. https://doi.org/10.1002/bit.24888

Kotlarz D, Buc H (1982) Phosphofructokinases from *Escherichia coli*. Methods Enzymol 90(Pt E):60–70

Kozlov YI, Chinen A, Izui H, Hara Y, Yasueda H, Rybak KV, Slivinskaya EA, Katashkina JY, Kozlov Y, Katashikina JY, Hisashi Y, Chinen AAC, Izui HAC, Hara YAC, Yasueda HAC (2006) New bacterium, which is modified to have an increased activity of D-xylulose-5-phosphate phosphoketolase and/or fructose-6-phosphate phosphoketolase, useful for producing useful metabolites, e.g. L-glutamic acid or L-proline. WO2006016705-A1

Krusemann JL, Lindner SN, Dempfle M, Widmer J, Arrivault S, Debacker M, He H, Kubis A, Chayot R, Anissimova M, Marliere P, Cotton CAR, Bar-Even A (2018) Artificial pathway emergence in central metabolism from three recursive phosphoketolase reactions. FEBS J 285:4367–4377. https://doi.org/10.1111/febs.14682

Lee SM, Jellison T, Alper HS (2012) Directed evolution of xylose isomerase for improved xylose catabolism and fermentation in the yeast *Saccharomyces cerevisiae*. Appl Environ Microbiol 78(16):5708–5716. https://doi.org/10.1128/aem.01419-12

Liu Q, Ouyang SP, Kim J, Chen GQ (2007) The impact of PHB accumulation on L-glutamate production by recombinant *Corynebacterium glutamicum*. J Biotechnol 132(3):273–279. https://doi.org/10.1016/jjbiotec.2007.03.014

Liu B, Peng Q, Sheng M, Hu S, Qian M, Fan B, He J (2018) Directed evolution of sulfonylurea esterase and characterization of a variant with improved activity. J Agric Food Chem 67:836–843. https://doi.org/10.1021/acs.jafc.8b06198

Meile L, Rohr LM, Geissman TA, Herensperger M, Teuber M (2001) Characterization of the D-xylulose 5-phosphate/D-Fructose 6-phosphate phosphoketolase gene (xfp) from *Bifidobacterium lactis*. J Bacteriol 183(9):2929–2936. https://doi.org/10.1128/jb.183.9.2929-2936.2001

Miyazaki K, Takenouchi M (2002) Creating random mutagenesis libraries using megaprimer PCR of whole plasmid. Biotechniques 33(5):1033–1038

Niebisch A, Bott M (2001) Molecular analysis of the cytochrome bc1-aa3 branch of the *Corynebacterium glutamicum* respiratory chain containing an unusual diheme cytochrome c1. Arch Microbiol 175(4):282–294

Nissler K, Otto A, Schellenberger W, Hofmann E (1983) Similarity of activation of yeast phosphofructokinase by AMP and fructose-2,6-bisphosphate. Biochem Biophys Res Commun 111(1):294–300

Orban JI, Patterson JA (2000) Modification of the phosphoketolase assay for rapid identification of *Bifidobacteria*. J Microbiol Methods 40(3):221–224. https://doi.org/10.1016/s0167-7012(00)00133-0

Pan J, Wu F, Wang J, Yu LQ, Khayyat NH, Stark BC, Kilbane JJ (2013) Enhancement of desulfurization activity by enzymes of the *Rhodococcus* dsz operon through coexpression of a high sulfur peptide and directed evolution. Fuel 112:385–390. https://doi.org/10.1016/j.fuel.2013.04.065

Peyret JL, Bayan N, Joliff G, Gulik-Krzywicki T, Mathieu L, Schechter E, Leblon G (1993) Characterization of the *cspB* gene encoding PS2, an ordered surface-layer protein in *Corynebacterium glutamicum*. Mol Microbiol 9(1):97–109

Posthuma CC, Bader R, Engelmann R, Postma PW, Hengstenberg W, Pouwels PH (2002) Expression of the xylulose 5-phosphate phosphoketolase gene, *xpkA*, from *Lactobacillus pentosus* MD363 is induced by sugars that are fermented via the phosphoketolase pathway and is repressed by glucose mediated by CcpA and the mannose phosphoenolpyruvate phosphotransferase system. Appl Environ Microbiol 68(2):831–837. https://doi.org/10.1128/aem.68.2.831-837.2002

Ruan YL, Zhu LJ, Li Q (2015) Improving the electro-transformation efficiency of *Corynebacterium glutamicum* by weakening its cell wall and increasing the cytoplasmic membrane fluidity. Biotechnol Lett 37(12):2445–2452. https://doi.org/10.1007/s10529-015-1934-x

Schafer A, Tauch A, Jager W, Kalinowski J, Thierbach G, Puhler A (1994) Small mobilizable multipurpose cloning vectors derived from the *Escherichia coli* plasmids pK18 and pK19 - selection of defined deletions in the chromosome of *Corynebacterium glutamicum*. Gene 145(1):69–73. https://doi.org/10.1016/0378-1119(94)90324-7

Servinsky MD, Germane KL, Liu S, Kiel JT, Clark AM, Shankar J, Sund CJ (2012) Arabinose is metabolized via a phosphoketolase pathway in *Clostridium acetobutylicum* ATCC 824. J Ind Microbiol Biotechnol 39(12):1859–1867. https://doi.org/10.1007/s10295-012-1186-x

Sgorbati B, Lenaz G, Casalicchio F (1976) Purification and properties of two fructose-6-phosphate phosphoketolases in *Bifidobacterium*. Antonie Van Leeuwenhoek 42(1-2):49–57

Sonderegger M, Schumperli M, Sauer U (2004) Metabolic engineering of a phosphoketolase pathway for pentose catabolism in *Saccharomyces cerevisiae*. Appl Environ Microbiol 70(5):2892–2897. https://doi.org/10.1128/aem.70.5.2892-2897.2004

Strandberg L, Enfors SO (1991) Factors influencing inclusion body formation in the production of a fused protein in *Escherichia coli*. Appl Environ Microbiol 57(6):1669–1674

Suzuki R, Katayama T, Kim BJ, Wakagi T, Shoun H, Ashida H, Yamamoto K, Fushinobu S (2010a) Crystal structures of phosphoketolase: thiamine diphosphate-dependent dehydration mechanism. J Biol Chem 285(44):34279–34287. https://doi.org/10.1074/jbc.M110.156281

Suzuki R, Kim BJ, Shibata T, Iwamoto Y, Katayama T, Ashida H, Wakagi T, Shoun H, Fushinobu S, Yamamoto K (2010b) Overexpression, crystallization and preliminary X-ray analysis of xylulose-5-phosphate/fructose-6-phosphate phosphoketolase from *Bifidobacterium breve*. Acta Crystallogr Sect F Struct Biol Cryst Commun 66(Pt 8):941–943. https://doi.org/10.1107/S1744309110023845

Takahashi K, Tagami U, Shimba N, Kashiwagi T, Ishikawa K, Suzuki E (2010) Crystal structure of *Bifidobacterium Longum* phosphoketolase; key enzyme for glucose metabolism in *Bifidobacterium*. FEBS Lett 584(18):3855–3861. https://doi.org/10.1016/j.febslet.2010.07.043

van der Rest ME, Lange C, Molenaar D (1999) A heat shock following electroporation induces highly efficient transformation of *Corynebacterium glutamicum* with xenogeneic plasmid DNA. Appl Microbiol Biotechnol 52(4):541–545. https://doi.org/10.1007/s002530051557

Wang CY, Li Y, Gao ZW, Liu LC, Zhang MY, Zhang TY, Wu CF, Zhang YX (2018a) Establishing an innovative carbohydrate metabolic pathway for efficient production of 2-keto-L-gulonic acid in *Ketogulonicigenium robustum* initiated by intronic promoters.

Microb Cell Factories 17(1):81. https://doi.org/10.1186/s12934-018-0932-9

Wang Q, Xu J, Sun Z, Luan Y, Li Y, Wang J, Liang Q, Qi Q (2018b) Engineering an in vivo EP-bifido pathway in *Escherichia coli* for high-yield acetyl-CoA generation with low CO_2 emission. Metab Eng 51:79–87. https://doi.org/10.1016/j.ymben.2018.08.003

Wang Y, Cao GQ, Xu DY, Fan LW, Wu XY, Ni XM, Zhao SX, Zheng P, Sun JB, Ma YH (2018c) A Novel *Corynebacterium glutamicum* L-Glutamate Exporter. Appl Environ Microbiol 84(6):15. https://doi.org/10.1128/aem.02691-17

Welch P, Scopes RK (1981) Rapid purification and crystallization of yeast phosphofructokinase. Anal Biochem 112(1):154–157

Whitworth DA, Ratledge C (1977) Phosphoketolase in *Rhodotorula graminis* and Other Yeasts. J Gen Microbiol 102:397–401

Yang XY, Yuan QQ, Zheng YY, Ma HW, Chen T, Zhao XM (2016) An engineered non-oxidative glycolysis pathway for acetone production in *Escherichia coli*. Biotechnol Lett 38(8):1359–1365. https://doi.org/10.1007/s10529-016-2115-2

Yevenes A, Frey PA (2008) Cloning, expression, purification, cofactor requirements, and steady state kinetics of phosphoketolase-2 from *Lactobacillus plantarum*. Bioorg Chem 36(1-3):121–127. https://doi.org/10.1016/j.bioorg.2008.03.002

Zhang J, Liu YJ (2013) Computational studies on the catalytic mechanism of phosphoketolase. Comput Theor Chem 1025:1–7. https://doi.org/10.1016/j.comptc.2013.09.026

Publisher's note Springer Nature remains neutral with regard to jurisdictional claims in published maps and institutional affiliations.